LBNL-49227
Preprint

ERNEST ORLANDO LAWRENCE
BERKELEY NATIONAL LABORATORY

Effect of Secondary Structure on the Interactions of Peptide T4 LYS(11-36) in Mixtures of Aqueous Sodium Chloride and 2,2,2-Trifluoroethanol

Camille O. Anderson, Susanne Spiegelberg,
John M. Prausnitz, and Harvey W. Blanch

Chemical Sciences Division

October 2001

Submitted to
Protein Science

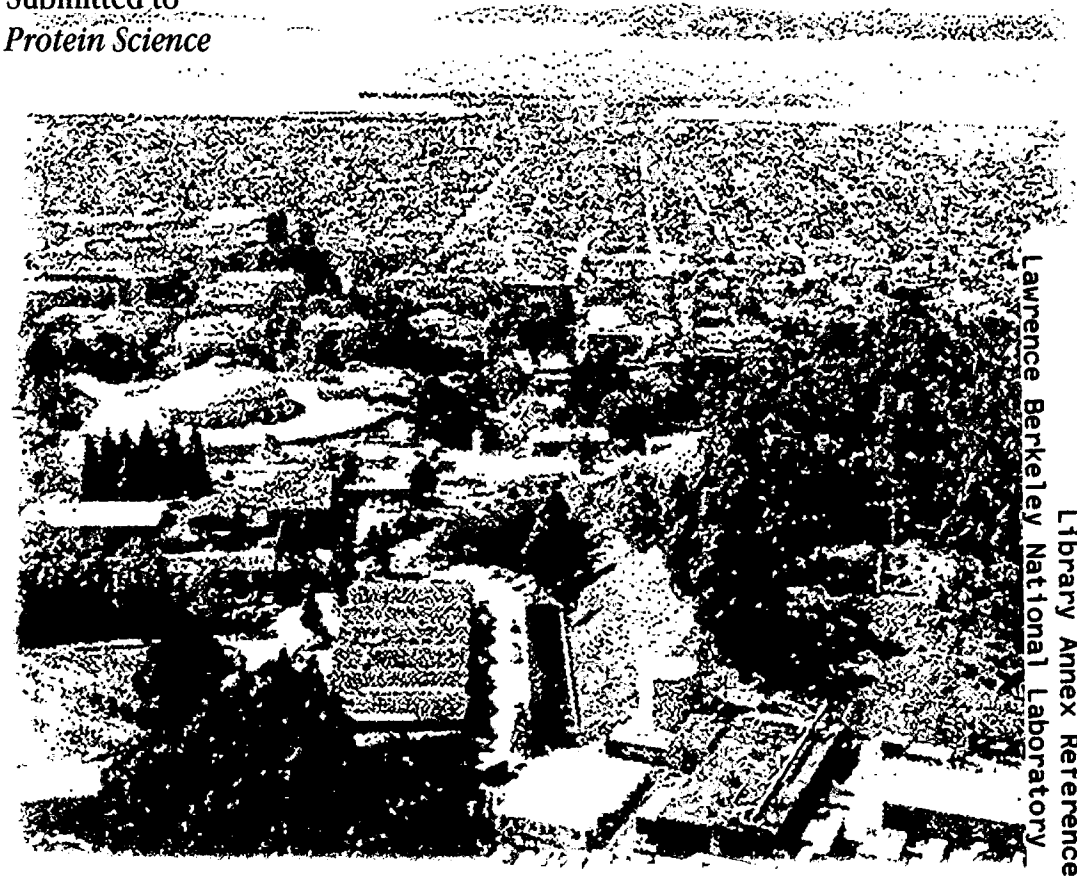

DISCLAIMER

LBNL-49227

Effect of Secondary Structure on the Interactions of Peptide T4 LYS(11-36) in Mixtures of Aqueous Sodium Chloride and 2,2,2-Trifluoroethanol

Camille O. Anderson,[1] Susanne Spiegelberg,[1,2]
John M. Prausnitz,[1,3] and Harvey W. Blanch[1]

[1]Department of Chemical Engineering
University of California, Berkeley, CA 94720

[2]Present Address: German Wool Research Institute
RWTH Aachen e.V.
Veltmanplatz 8
D-52062 Aachen, Germany

[3]Chemical Sciences Division
Ernest Orlando Lawrence Berkeley National Laboratory
University of California
Berkeley, California 94720

October 2001

This work was supported by the Director, Office of Science, Office of Basic Energy Sciences, Chemical Sciences Division, of the U.S. Department of Energy under Contract No. DE-AC03-76SF00098.

Abstract

The potential of mean force for protein-protein interactions is key to the development of a statistical-mechanical model for salt-induced protein precipitation and crystallization, and for understanding certain disease states, including cataract formation and β-amyloid pathology in Alzheimer's disease. Fluorescence anisotropy provides a method for quantitative characterization of intermolecular interactions due to reversible association. Monomer-dimer equilibria for the peptide T4 LYS(11-36) were studied by fluorescence anisotropy. This peptide, derived from the β-sheet region of the T4 lysozyme molecule, has the potential to form amyloid fibrils. 2,2,2-trifluoroethanol (TFE) induces a change in peptide secondary structure, and was used in aqueous solutions at concentrations from 0 to 50% (v/v) at 25 and 37°C to examine the role of peptide conformation on peptide-peptide interactions. The association constant for dimerization increased with rising TFE concentration and with falling temperature. The peptide-peptide potential of mean force was computed from these association constants. Circular-dichroism measurements showed that the secondary structure of the peptide plays an important role in these strong attractive interactions due to intermolecular hydrogen-bond formation and hydrophobic interactions.

Keywords: Protein-protein interactions; 2,2,2-trifluoroethanol; Potential of mean force; Fluorescence polarization; Fluorescence anisotropy; Amyloid fibrillogenesis; Circular dichroism; Secondary structure

Protein-protein interactions can be selectively enhanced to precipitate target proteins from fermentation processes and to crystallize proteins for characterization by X-ray diffraction. Optimized conditions for salt-induced protein precipitation and crystallization have typically been identified on a trial-and-error basis or through empirical correlations. Through measurements of protein-protein interactions under dilute-solution conditions, a molecular-thermodynamic model can be developed for predicting selective phase separation of proteins in aqueous electrolyte solutions.

Strongly attractive intermolecular interactions between proteins lead to a variety of disease states. The neurotoxicity in Alzheimer's disease has been hypothesized to arise from the association of monomers or dimers of Aβ protein to form protofibrils with β-sheet structure (Walsh et al., 1997; Harper et al., 1997; Shen and Murphy, 1995). These protofibrils lengthen to fibrils that form clusters. Amyloid plaques are observed in the brains of Alzheimer's victims. Human diseases that involve similar pathology include type II diabetes, hereditary systemic amyloidosis and Creutzfeldt-Jakob disease. Therefore, quantitative characterization of the intermolecular forces that produce protein aggregation may lead to a better understanding of the origin of these diseases.

This work is concerned with protein-protein interactions that may be related to β-amyloid formation. Several variants of lysozyme provide a model of amyloid fibrillogenesis. A peptide fragment from the β-sheet region of hen egg-white lysozyme forms extensive intermolecular β-structure at low pH (Yang et al., 1994). Hen egg-white lysozyme in ethanol:water mixtures (Goda et al., 2000) and human lysozyme mutants (Booth et al., 1997) also demonstrate amyloidogenic properties.

In the present work, the intermolecular interactions that lead to β-amyloid fibrillogenesis are examined using fluorescence-anisotropy measurements of the peptide T4 LYS(11-36), a 26 amino-acid peptide derived from the β-sheet region of T4 lysozyme, in mixtures of aqueous sodium chloride and TFE. With fluorescence anisotropy, changes in the association state of molecules are reflected by changes in rotational Brownian motion. The anisotropy increases with degree of association. In general, TFE is used to denature proteins and to stabilize secondary structures in peptides. In aqueous solutions containing increasing TFE concentrations, T4 LYS(11-36) has been shown to undergo a secondary-structure transition from random coil to β-sheet to α-helix (Najbar et al., 1997). Because the secondary structure of a peptide can play a role in intermolecular interactions, the secondary structure of T4 LYS(11-36) is determined from circular-dichroism (CD) spectropolarimetry in solution conditions similar to those used for fluorescence-anisotropy measurements.

The two-body interactions between peptide molecules are quantified through a potential of mean force composed of a repulsive hard-sphere potential, an attractive dispersion potential, an electric double-layer-repulsion potential, and an attractive site-specific square-well potential.

Results

Fluorescence anisotropy

The anisotropy of T4 LYS(11-36) was measured in 25-mM sodium phosphate buffer containing 0.16 M NaCl at pH 4. TFE concentrations ranged from 0 to 50% (v/v). The total peptide concentration, $[\Lambda]_T$, was varied in the range 0.5 to 50 μM. Measurements performed at 25 and 37°C are shown in Figures 1 and 2, respectively. At 0% TFE, the anisotropy increases slightly with rising peptide concentration indicating that little binding occurs under these solution

conditions. As the concentration of TFE increases, the anisotropy becomes a stronger function of concentration, indicating increased binding.

Association constant and potential of mean force

TFE induces a change in secondary structure as measured by circular-dichroism spectropolarimetry described below. This change affects the molecular volume of the peptide. The structural change may also affect the angle between the absorption and emission dipoles of the fluorophore (Lakowicz, 1999). As a result, A_f (the infinite-dilution anisotropy) and A_b (the limiting value at high peptide concentrations where all molecules are in the bound form) vary with TFE concentration, as shown in Tables 1 and 2. Temperature also affects the anisotropy. We correct for the effect of temperature on viscosity as described by Anderson et al. (2000). However, there is also a direct dependence on temperature, and a temperature dependence that is manifested by changes in the molecular volume (Perrin, 1926). Thus, A_f and A_b also vary with temperature (Tables 1 and 2).

Association constants for dimerization of T4 LYS(11-36) are calculated by fitting the experimental data to Equation (2). The best-fit curves are shown in Figures 1 and 2. Figure 3 shows that the association constant increases with TFE concentration and decreases with temperature.

The potential of mean force is calculated from the association constant using Equations (3)-(5). Figure 4 shows that the well depth of the specific-interaction potential, ε_{spec}, increases as the TFE content rises. At low TFE concentration, the well depth decreases with temperature. At 50% (v/v) TFE, there is no significant temperature effect.

CD spectropolarimetry

CD spectra were obtained as a function of TFE content at 25°C, with peptide concentrations ranging from 21 to 26 μM. Results are shown in Figure 5. The CD spectrum in TFE-free salt solution has a minimum at 197 nm, consistent with the peptide having a random-coil conformation (Woody, 1996). At a TFE concentration of 50% (v/v), the spectrum has a minimum at 208 nm, and significant negative ellipticity at 222 nm, indicating that the peptide has a considerable amount of helical structure. At intermediate TFE concentrations, the spectra indicate β-structure. These spectra are similar to that obtained by Najbar et al. (1997) at pH 4.8 in 10-mM potassium phosphate buffer.

Figure 5 also shows fits for the spectra using the reference data set of Brahms and Brahms (1980). Figure 6 shows the extent of secondary structure obtained from these fitted spectra. As the TFE content rises to 20%, the β-sheet content increases from 26 to 38%. The total β content ranges from 43 to 48%. But with an increase to 50% TFE, the β-sheet content (and total β content) drops to 15%, and the α-helical content increases from 0 to 60%.

Structure Prediction

Tables 3 and 4 show the secondary structure of T4 LYS(11-36) as predicted by the ALB program (Ptitsyn and Finkelstein, 1983). These predictions, based on the amino-acid sequence of the peptide, were made at 25 and 37°C, using charged termini at pH 4 and 0.16 M NaCl. An aqueous environment was used to represent the 0% TFE condition. The intermediate TFE concentrations were simulated using the partially hydrophobic environment. The fully hydrophobic condition was used to mimic 50% TFE, based on the suggestion by Jasanoff and Fersht (1994) that complete helicity is generally reached at 50% TFE.

At both temperatures, the peptide is predicted to have high β-strand content at aqueous and partially hydrophobic conditions. However, high α-helical content is predicted under fully hydrophobic conditions. Tables 5 and 6 show the percentage of α-helical and β-strand content at each set of solution conditions. The peptide is predicted to be as much as 46% β-strand in aqueous and partially hydrophobic solutions, while it is up to 62% α-helix when the solution is fully hydrophobic.

Discussion

Strength and Nature of Interaction

The attractive forces that drive interactions between these peptide molecules are those observed for various proteins known to undergo amyloid fibrillogenesis. The observed well depth of the specific-interaction potential, ε_{spec}, is in the range 16-19 kT (Figure 4). At 25°C, this corresponds to bond energies on the order of 39-47 kJ/mol. At 37°C, the corresponding bond energies are 41-49 kJ/mol. The strength of a hydrogen bond is approximately 13-30 kJ/mol (Stryer, 1988), while the free energy of dimerization for a hydrophobic molecule with a diameter of 18.8 Å is -38 kJ/mol (Israelachvili and Pashley, 1982).

It is possible that the attractive interaction is due to the formation of intermolecular hydrogen bonds. All amino acids can form main-chain/main-chain hydrogen bonds. The side chains of serine and threonine can form both local and long-range hydrogen bonds with main-chain C=O and NH groups (Baker and Hubbard, 1984). Asparagine and glutamine generally form non-local hydrogen bonds with the main chain. Aspartic acid and glutamic acid act as hydrogen-bond acceptors for main-chain NH groups. Because lysine and arginine are long and flexible, they typically form long-range intramolecular and intermolecular hydrogen bonds. In general, histidine forms local hydrogen bonds with the main chain, while tyrosine forms long-

range hydrogen bonds. There are 15 amino acids in T4 LYS(11-36) whose side chains can hydrogen bond with the main chain (Materials and methods section).

Hydrophobic bonds could also contribute to the strong attraction. There are 14 amino acids in the T4 LYS(11-36) sequence that can participate in hydrophobic interactions (Materials and methods section).

Dependence of structure and interactions on TFE concentration

As TFE concentration increases, the T4 LYS(11-36) peptide undergoes a random-coil to β-strand to α-helix transition while experiencing increased intermolecular attraction (Figures 5 and 6). A peptide corresponding to the β-sheet region of hen egg-white lysozyme, residues 41-60, undergoes a similar secondary-structure transition in TFE (Yang et al., 1994). Various alcohols cause a similar transition in the secondary structure of poly(L-lysine) (Shibata et al., 1992). Although these peptides are predominantly helical at high TFE concentrations, there are preexisting conformational preferences that must first be overcome before they can achieve helicity (Buck, 1998). The secondary-structure predictions (Tables 3-6) show that the T4 LYS(11-36) peptide has a high propensity for β-sheet structure in aqueous and partially hydrophobic environments, suggesting that, at moderately low cosolvent concentrations, β rather than α-structure may be stabilized. At higher concentrations, a strong propensity for α-helix is observed.

There are several proposed mechanisms for the effect of TFE on proteins and peptides. TFE in aqueous solution may (1) increase the solvent structure, (2) preferentially hydrogen bond to the carbonyl oxygens in the polypeptide chain, and (3) interact with the hydrophobic amino-acid sidechains.

Light-scattering intensities show a maximum at 50% (v/v) TFE, suggesting a change in water structure (Gast et al., 1999). From these dynamic light-scattering measurements, Gast and coworkers concluded that alcohol-water clathrates form, and that the sizes of these clathrates, as well as the ratio of TFE molecules to water molecules, depend on TFE concentration.

Llinás and Klein (1975) have demonstrated that TFE is significantly less basic than water. Therefore, TFE is a slightly stronger proton donor than water, but a much weaker proton acceptor. Adding TFE to the salt solution decreases the ability of the solvent to compete with peptide carbonyl acceptors, and decreases the ability of amide protons to form hydrogen bonds with the solvent. This encourages the formation of hydrogen bonds between peptide-amide donors and peptide-carbonyl acceptors (Thomas and Dill, 1993). For T4 LYS(11-36), at low TFE concentrations, intermolecular hydrogen bonds are formed, whereas intramolecular hydrogen bonds are preferred at high TFE concentrations (Figures 5 and 6).

It has been shown that TFE molecules associate with hydrophobic sites on the protein surface (Yang et al., 1993). The addition of TFE also reduces the interaction between hydrophobic side chains in a peptide (Albert and Hamilton, 1995). Because hydrophobic interactions are important for the stabilization of β-sheet structures (Mutter and Altman, 1985), we expect a decrease in β-sheet content with an increase in TFE concentration, as observed for T4 LYS(11-36). Also, the formation of alcohol-water clathrates results in a high local concentration of TFE relative to that in bulk solution, and may affect hydrophobic interactions.

Based on these observations, Reiersen and Rees (2000) developed a model to explain the effect of TFE on the secondary structure of proteins and peptides. At low alcohol concentrations (0-10% v/v), where the TFE clusters are not fully developed or stabilized, TFE draws water away from the surface of proteins. As the TFE concentration increases and the cluster size

becomes larger, the clusters may associate directly with hydrophobic side chains. This decreases the side-chain conformational entropy; that decrease may be important in the formation of α-helices (Aurora et al., 1997). When the bulk concentration of TFE is above 50%(v/v), the TFE clusters are smaller, but have a higher local intra-cluster TFE concentration. This enables non-local side chain interactions in a peptide to become more localized. Generally, TFE induces transitions from a non-local (β-sheet) to a local folding nucleus (helices, turns, hairpins).

In the context of the cluster model of Reiersen and Rees, the TFE-induced secondary-structure transition of T4 LYS(11-36) can be easily explained. However, the change in the strength of interaction is unusual. At low TFE concentrations, where non-local contacts (β-sheet) are stabilized, the strength of intermolecular attraction increases, as expected (Figures 3 and 4). However, at high TFE concentrations the strength of protein-protein hydrophobic interactions is expected to decrease. Also, the induction of α-helical conformation should reflect a decrease in the number of protein-protein intermolecular hydrogen bonds. Overall, we expect a decrease in the strength of attraction between T4 LYS(11-36) molecules to accompany the increase in helical content at high TFE concentrations. However, we observe an increase in intermolecular attraction (Figures 3 and 4).

A similar phenomenon is observed for two peptides, derived from human apolipoproteins C-II and E, in 30% (v/v) TFE (MacPhee et al., 1997). Helical formation is accompanied by the formation of discrete helix coil-coil dimers and trimers, respectively. These peptides are predicted to form amphipathic helices, and they present a hydrophobic face to the lipid surface. It is possible that clusters of TFE cooperatively associate with the hydrophobic surface of a helix. In this manner, the clusters mimic the environment of a membrane or the interior of a protein, enabling the helices to aggregate. Although T4 lysozyme is not a membrane protein, 38% of the

residues in T4 LYS(11-36) are hydrophobic. Thus, a similar mechanism may increase intermolecular attraction as observed with increased α-helical content of this peptide.

Temperature dependence of interaction

The strength of the specific interaction is a weak function of temperature at 0 and 20% (v/v) TFE, whereas at 10% TFE, it is a mildly stronger function of temperature (Figure 4). At 50% TFE, the interaction is independent of temperature.

Results from Rothemund and coworkers (1996) suggest that, as temperature rises, there is a disruption of intermolecular hydrogen bonds between protein carbonyl groups and TFE in TFE:water mixtures. In T4 LYS(11-36), such a disruption of TFE-peptide hydrogen bonds may lead to the formation of intermolecular peptide-peptide hydrogen bonds as the peptide tries to fulfill its hydrogen-bonding potential. Hydrophobic attraction is also expected to increase with temperature (Claesson et al., 1986). Therefore, if the TFE-induced attraction were due solely to hydrogen-bond formation and hydrophobic interactions between peptide molecules, we would expect more attraction as temperature rises in TFE:water mixtures. However, the square-well depth, ε_{spec}, is unaffected by changes in temperature at 50% TFE. We therefore conclude that while hydrophobic interactions and hydrogen-bond formation play a role in TFE-induced attraction, there are additional forces that are not taken into account.

Accuracy of interaction measurements

There is considerable scatter in the fluorescence-anisotropy data. As the solutions were diluted from a total peptide concentration of 50 μM to 0.5 μM, the data became more scattered. In general, to avoid excessive scatter, one should keep the total fluorescence intensity constant throughout the experiment. However, we were unable to achieve this because our more important goal was to maintain the 1:20 ratio of labeled to unlabeled peptide throughout the

experiment (Materials and methods section). Without this requirement the system of equations would have been underdetermined and it would have been impossible to calculate the association constant (Anderson et al., 2000). Therefore, the majority of the error in the fluorescence-anisotropy measurements was due to serial dilution and the resulting decrease in total fluorescence intensity.

Another source of error is the assumption of a spherical molecule under all solution conditions. From the circular-dichroism measurements, we know that the secondary structure changes with TFE concentration. Thus, the assumption of a hard sphere may produce some error. It may be more accurate to model the molecules as rods rather than as spheres when the molecule is predominantly β-sheet or α-helical. The assumption of a spherical molecule affects the potential of mean force calculation, as well as the viscosity correction of the anisotropy results.

Error is also introduced by assuming that the highest oligomer formed is a dimer. If higher oligomers were formed, the cutoff distance for the specific interaction potential would have to be altered. The calculated association constant would also be affected.

Conclusions

This work describes interactions of the peptide T4 LYS(11-36) in mixtures of aqueous sodium chloride and 2,2,2-trifluoroethanol. Understanding the factors that affect protein-protein interactions provides insight into the molecular basis for amyloid fibrillogenesis, as well as for salt-induced separation of proteins. To provide a better understanding of these phenomena, the specific forces that act between proteins and peptides must be understood. The interactions that contribute to the potential of mean force cannot be described by simple DLVO theory. In peptides, hydrophobic interactions and the formation of hydrogen bonds contribute significantly to the overall intermolecular interaction.

Materials and methods

Peptide synthesis

T4 LYS(11-36) was assembled by Fmoc-solid phase synthesis on an Applied Biosystems 431A synthesizer, using previously described methodology (Anderson et al., 2000). The amino-acid sequence is EGLRLKIYKDTEGYYTIGIGHLLTKS. The lyophilized peptide powder contained approximately 1 mole TFA (trifluoroacetic acid) per positive charge and 20% H_2O. Electrospray ionization mass spectrometry yielded a molecular weight of 2969.4 Da, consistent with the theoretical value. The peptide isoelectric point is 9.9.

Conjugation of fluorescent label

Because the T4 LYS(11-36) peptide does not have significant intrinsic fluorescence, it is labeled with an extrinsic fluorophore. 7-Methoxycoumarin-3-carboxylic acid (Molecular Probes, Inc., Eugene, Oregon, cat# M-1420) was attached to the N-terminus of the peptide as discussed previously (Anderson et al., 2000). Addition of this fluorescent label resulted in a molecular weight of 3171.7 Da, as measured by electrospray ionization mass spectrometry.

Sample preparation

Buffer solutions were prepared as described previously (Anderson et al., 2000). Peptide solutions for fluorescence-anisotropy measurements were prepared such that the mole ratio of fluorescently labeled to unlabeled peptide was approximately 1:20. This ratio was chosen to ensure sufficient fluorescent signal for measurement, while minimizing fluorescence transfer. Peptide solutions with a concentration of 50 μM were prepared in 2 ml of 25-mM sodium-phosphate buffer at pH 4. The solutions were then dialyzed overnight against 1 L of 25-mM sodium phosphate buffer at pH 4 containing isotonic sodium chloride (0.16 M). Dialysis resulted in both solvent exchange and dilution of the contaminant trifluoroacetic acid (TFA), which is

used in peptide purification. After dialysis, the pH was adjusted to the desired value using either $1x10^{-4}$ M phosphoric acid or $1x10^{-4}$ M sodium hydroxide. The 50-μM peptide solution was diluted with buffer to obtain solutions in the concentration range 0.5 to 50 μM. The desired amount of TFE (0, 10, 20 or 50% v/v) was then added to each solution. The solutions were allowed to equilibrate for one hour before the anisotropy was measured.

Fluorescence-anisotropy measurements

In the fluorescence-anisotropy technique, a fluorophore is excited with vertically polarized light at a given wavelength (Bentley et al., 1985; Lakowicz, 1999). When the polarized light impinges on the sample, it can be depolarized in several ways; here we focus on depolarization by rotation of molecules. The fluorescence intensity of light emitted from the fluorophore is measured at a higher wavelength, in two directions: parallel to and perpendicular to the direction of polarization of the incident light. The difference gives a measure of the amount of depolarization that has occurred. The anisotropy is defined as (Perrin, 1926):

$$A = \frac{I_{II} - I_{\perp}}{I_{II} + 2I_{\perp}} \qquad (1)$$

where I_{II} is the intensity of emitted light measured in the direction parallel to excitation, and $I_{\perp}$ is the intensity of light measured in the direction perpendicular to excitation. The sum in the denominator is the total fluorescence intensity.

Fluorescence anisotropy was measured on a Beacon® 2000 Fluorescence Polarization System from Panvera Corporation, using filters with maximum transmissions at 360±10 nm and 400 ±10 nm. (The excitation and emission maxima for the coumarin-labeled peptide were found to be 360 nm and 404 nm, respectively.) Measurements were obtained at 25°C and 37°C.

Because the solution viscosity changes upon addition of TFE (Palepu and Clark, 1989), the anisotropy was corrected in the manner described by Anderson et al. (2000). The viscosity increase due to the salt was neglected because it was less than 2 % (Wolf et al., 1986), compared with a 111 % viscosity increase for the 50 volume % TFE solution (Palepu and Clark, 1989).

Association constant

The association constant for dimerization, K_a, is determined by measuring the anisotropy as a function of peptide concentration. Non-linear least-squares analysis is used to fit the anisotropy versus concentration data to the equation (Anderson et al., 2000):

$$[\Lambda]_T = \frac{\left[\left(\frac{A-A_f}{A_b-A_f}\right)+\left(\frac{A-A_f}{A_b-A_f}\right)^2\right]}{K_a\cdot\left[1-\left(\frac{A-A_f}{A_b-A_f}\right)\right]^2\cdot\left[\lambda-\left(\frac{A-A_f}{A_b-A_f}\right)\lambda^*\right]} \qquad (2)$$

where $[\Lambda]_T = [L]_T + [L^*]_T$ is the total molar peptide concentration. $[L]_T$, the total molar concentration of unlabeled peptide, and $[L^*]_T$, the total concentration of labeled peptide, are measured spectroscopically, as described previously (Anderson et al., 2000). In Equation (2), λ^* is the mole fraction of labeled peptide and λ is the mole fraction of unlabeled peptide. The anisotropy of the free state, A_f, is obtained experimentally by measuring the anisotropy of increasingly dilute peptide solutions. When the anisotropy value no longer decreases upon dilution, that value is taken as the anisotropy of the free peptide. The anisotropy of the bound state, A_b, is estimated by plotting the experimental anisotropy as a function of log $[\Lambda]_T$, and extrapolating to infinite concentration.

Potential of mean force

For a spherically-symmetric potential of mean force, $W(r)$, the association constant is given by the volume integral (Chandler, 1987):

$$K_a = \frac{1}{2}\int_{\sigma}^{\sigma+x_c} \exp\left[-W(r)/kT\right]\cdot 4\pi r^2 dr \qquad (3)$$

where σ =18.8 Å is the effective spherical diameter of the hydrated peptide (Anderson et al., 2000). The cutoff distance, x_c, refers to the specific-interaction potential.

The potential of mean force for this peptide is given as the sum of four spherically symmetric pairwise potentials:

$$W(r) = W_{hs}(r) + W_{elec}(r) + W_{disp}(r) + W_{spec}(r) \qquad (4)$$

where $W_{hs}(r)$ is the hard-sphere potential, $W_{elec}(r)$ is the electric double-layer-repulsion potential, and $W_{disp}(r)$ is the dispersion potential. The first three terms of Equation (4) constitute the potential of mean force in Derjaguin-Landau-Verwey-Overbeek (DLVO) theory (Verwey and Overbeek, 1948). The forms of these potentials are given in Anderson et al. (2000). The valence of the peptide, z, is +3.1 at pH 4 (Anderson et al. 2000), and the relative dielectric permittivity of the solvent, ε_r, was obtained from Murto and Heino (1966). These parameters are used in the electric double-layer-repulsion potential. The Hamaker constant, H, used in the dispersion potential, is 5 kT.

$W_{spec}(r)$ is a site-specific orientation-dependent potential that accounts for intermolecular attraction due to hydrophobic forces, hydrogen-bond formation, or short-range attractive electrostatic forces (Curtis et al., 1998). This potential arises between the attractive site of one molecule and that on another, and is given by the square-well model (Wertheim, 1986):

$$\phi(r) = \begin{cases} -\varepsilon_{spec} & for \quad x < x_c \\ 0 & for \quad x > x_c \end{cases} \tag{5}$$

where x is the distance between the sites and $x_c = 0.134\sigma$ is the cutoff distance of the attractive potential (Wertheim, 1986). This cutoff distance is used to ensure that only dimers are formed. The spherically symmetric potential $W_{spec}(r)$ is obtained by calculating the orientation average of $\phi(r)$. In this work, the depth of the square well, ε_{spec}, is a fitting parameter, calculated from experimental K_a.

CD spectropolarimetry

Unlabeled-peptide solutions were prepared in 50-mM sodium-phosphate buffer at pH 4 and dialyzed overnight against 0.16 M NaCl solution at pH 4; TFE was added in the appropriate amount. Final peptide concentrations were between 21 and 26 μM. CD spectra were recorded at 25°C on an Aviv Model 62DS circular-dichroism spectropolarimeter using a 2-mm pathlength cuvette. The wavelength range was 190-250 nm, with intervals of 0.5 nm and a bandwidth of 1.5 nm. Mean molar ellipticities (degree-cm^2/dmol-residue) are reported here.

Deconvolution of the CD spectra and estimation of the secondary-structure content were accomplished by using constrained linear least squares analysis and the reference spectra of Brahms and Brahms (1980).

Secondary structure prediction

The ALB program (Ptitsyn and Finkelstein, 1983) was used to predict the conformational preferences of the T4 LYS(11-36) peptide from its amino-acid sequence. This program can be used to predict secondary structure based on the physicochemical properties of peptides and their environment.

Acknowledgements

This work was supported by the National Science Foundation under Grant Number CTS 9530793, and by the Director, Office of Science, Office of Basic Energy Sciences Chemical Sciences Division of the US Department of Energy under Contract Number DE-AC03-76SF00098. We thank Dr. David King for the synthesis, purification and analysis of the unlabeled and labeled peptides. The authors also acknowledge the contributions of Professor Susan Marqusee.

References

Albert, J.S. and Hamilton, A.D. 1995. Stabilization of helical domains in short peptides using hydrophobic interactions. *Biochemistry* **34:** 984-990.

Anderson, C.O., Niesen, J.F.M., Blanch, H.W., and Prausnitz, J.M. 2000. Interactions of proteins in aqueous electrolyte solutions from fluorescence-anisotropy measurements and circular-dichroism measurements. *Biophys. Chem.* **84:** 177-188.

Aurora, R., Creamer, T.P., Srinivasan, R., and Rose, G.D. 1997. Local interactions in protein folding: Lessons from the α-helix. *J. Biol. Chem.* **272:** 1413-1416.

Baker, E.N. and Hubbard, R.E. 1984. Hydrogen bonding in globular proteins. *Prog. Biophys. Mol. Biol.* **44:** 97-179.

Bentley, K.L., Thompson, L.K., Klebe, R.J., and Horowitz, P.M. 1985. Fluorescence polarization: A general method for measuring ligand binding and membrane microviscosity. *BioTechniques* **3:** 356-366.

Booth, D.R., Sunde, M.. Bellotti V., Robinson, C.V., Hutchinson, W.L., Fraser, P.E., Hawkins, P.N., Dobson, C.M., Radford, S.E., Blake, C.C.F., and Pepys, M.B. 1997. Instability, unfolding and aggregation of human lysozyme variants underlying amyloid fibrillogenesis. *Nature* **385:** 787-793.

Brahms, S. and Brahms, J. 1980. Determination of protein secondary structure in solution by vacuum ultraviolet circular dichroism. *J. Mol. Biol.* **138:** 149-178.

Buck, M. 1998. Trifluoroethanol and colleagues: Cosolvents come of age. Recent studies with peptides and proteins. *Quart. Rev. Biophys.* **31:** 297-355.

Chandler, D. 1987. *Introduction to modern statistical mechanics*, pp. 211-212. Oxford University Press, New York, NY.

Claesson, P.M., Kjellander, R., Stenius, P., and Christenson, H.K. 1986. Direct measurement of temperature-dependent interactions between non-ionic surfactant layers. *J. Chem. Soc. Faraday Trans. I* **82:** 2735-2746.

Curtis, R.A., Prausnitz, J.M., and Blanch, H.W. 1998. Protein-protein and protein-salt interactions in aqueous protein solutions containing concentrated electrolytes. *Biotechnol. Bioeng.* **57:** 11-21.

Gast, K., Zirwer, D., Müller-Frohne, M. and Damaschun, G. 1999. Trifluoroethanol-induced conformational transitions of proteins: Insights gained from the differences between α-lactalbumin and ribonuclease A. *Protein Sci.* **8:** 625-634.

Goda, S., Takano, K., Yamagata, Y., Nagata, R., Akutsu, H., Maki, S., Namba, K., and Yutani, K. 2000. Amyloid protofilament formation of hen egg lysozyme in highly concentrated ethanol solution. *Protein Sci.* **9:** 369-375.

Harper, J.D., Lieber, C.M., and Lansbury, P.T. 1997. Atomic force microscopic imaging of seeded fibril formation and fibril branching by the Alzheimer's disease amyloid β-protein. *Chem. Biol.* **4:** 951-959.

Israelachvili, J. and Pashley, R. 1982. The hydrophobic interaction is long range, decaying exponentially with distance. *Nature* **300:** 341-342.

Jasanoff, A. and Fersht, A.R. 1994. Quantitative determination of helical propensities from trifluoroethanol titration curves. *Biochemistry* **33:** 2129-2135.

Lakowicz, J.R. 1999. *Principles of fluorescence spectroscopy*, 2nd ed., Chapter 10. Kluwer Academic/Plenum Publishers, New York, NY.

Llinás, M. and Klein, M.P. 1975. Charge relay at the peptide bond. A proton magnetic resonance study of solvation effects on the amide electron density distribution. *J. Am. Chem. Soc.* **97:** 4731-4737.

MacPhee, C.E., Perugini, M.A., Sawyer W.H., and Howlett, G.J. 1997. Trifluoroethanol induces the self-association of specific amphipathic peptides. *FEBS Lett.* **416:** 265-268.

Murto, J. and Heino, E.-L. 1966. Fluoroalcohols. Part 1. Densities, partial molar volumes, Viscosities, and dielectric constants of 2,2,2-trifluoroethanol-water mixtures. *Suom. Kemistil. B* **39:** 263-266.

Mutter, M. and Altmann, K.-H. 1985. Sequence-dependence of secondary structure formation II. *Int. J. Pep. Prot. Res.* **26:** 373-380.

Najbar, L.V., Craik, D.J., Wade, J.D., Salvatore, D., and McLeish, M.J. 1997. Conformational analysis of LYS(11-36), a peptide derived from the β-sheet region of T4 lysozyme, in TFE and SDS. *Biochemistry* **36:** 11525-11533.

Palepu R. and Clarke, J. 1989. Viscosities and densities of 2,2,2-trifluoroethanol + water at various temperatures. *Thermochim. Acta* **156:** 359-363.

Perrin, M.F. 1926. Polarisation de la lumiére de fluorescence. Vie moyenne des molécules dans l'état excité. *J. Phys. Radium* **6/7:** 390-401.

Ptitsyn O.B., and Finkelstein, A.V. 1983. Theory of protein secondary structure and algorithm of its prediction. *Biopolymers* **22:** 15-25.

Reiersen, H. and Rees, A.R. 2000. Trifluoroethanol may form a solvent matrix for assisted hydrophobic interactions between peptide side chains. *Protein Eng.* **13:** 739-743.

Rothemund, S., Weiβhoff, H., Beyermann, M., Krause, E., Bienert, M., Mügge, C., Sykes, B.D., and Sönnichsen, F.D. 1996. Temperature coefficients of amide proton NMR resonance

frequencies in trifluoroethanol: A monitor of intramolecular hydrogen bonds in helical peptides? *J. Biomolecular NMR* **8:** 93-97.

Shen, C.-L. and Murphy, R.M. 1995. Solvent effects on self-assembly of β-amyloid protein. *Biophys. J.* **69:** 640-651.

Shibata, A., Yamamoto, M., Yamashita, T., Choiu, J.-S., Kamaya H., and Ueda, I. 1992. Biphasic effects of alcohols on the phase transition of poly(L-lysine) between α-helix and β-sheet conformations. *Biochemistry* **31:** 5728-5733.

Stryer, L. 1988. *Biochemistry*, 3rd ed., W.H. Freeman and Company, New York, NY.

Swiss Protein Database http://expasy.hcuge.ch/cgi-bin/protparam

Thomas, P.D. and Dill, K.A. 1993. Local and nonlocal interactions in globular proteins and mechanisms of alcohol denaturation. *Protein Sci.* **2:** 2050-2065.

Verwey, E.J.W. and Overbeek, J.T.K. 1948. *Theory of lyophobic colloids*, Elsevier, Amsterdam.

Walsh, D.M., Lomakin, A., Benedek, G.B., Condron, M.M., and Teplow, D.B. 1997. Amyloid β-protein fibrillogenesis: Detection of a protofibrillar intermediate. *J. Biol. Chem.* **272:** 22364-22372.

Wertheim, M.S. 1986. Fluids of dimerizing hard spheres and fluid mixtures of hard spheres and dispheres. *J. Chem. Phys.* **85:** 2929-2936.

Wolf, A.V. Brown, M.G., and Prentiss, P.G. 1986. Concentrative properties of aqueous solutions: Conversion tables. In *CRC handbook of chemistry and physics*, 67th ed. (ed. R.C. Weast) pp. D-253-D254. CRC Press, Inc., Boca Raton, FL.

Woody, R.W. 1996. Theory of circular dichroism of proteins. In: *Circular dichroism and the conformational analysis of biomolecules*, (ed. G.D. Fasman), Plenum Press, New York, NY.

Yang, J.J., Pitkeathly, M., and Radford, S.E. 1994. Far-UV circular dichroism reveals a conformational switch in a peptide fragment from the β-sheet of hen lysozyme. *Biochemistry* **33:** 7345-7353.

Yang, Y., Barker, S., Chen, M.J., and Mayo, K.H. 1993. Effect of low molecular weight aliphatic alcohols and related compounds on platelet factor 4 subunit association, *J. Biol. Chem.* **268:** 9223-9229.

Table 1. Anisotropy of the free and bound states for the T4 LYS(11-36) peptide in 0.16 M NaCl, pH 4 at 25°C.

% TFE (v/v)	A_f	A_b
0	0.06	0.15
10	0.07	0.14
20	0.08	0.13
50	0.01	0.13

Table 2. Anisotropy of the free and bound states for the T4 LYS(11-36) peptide in 0.16 M NaCl, pH 4 at 37°C.

% TFE (v/v)	A_f	A_b
0	0.06	0.18
10	0.06	0.13
20	0.08	0.13
50	0.02	0.13

Table 3. Secondary Structure Prediction for the T4 LYS(11-36) peptide in 0.16 M NaCl, pH 4 at 25°C.

	E	G	L	R	L	K	I	Y	K	D	T	E	G	Y	Y	T	I	G	I	G	H	L	L	T	K	S
aqueous					B	S	S	S	B	B	T	T	T	B	S	S	S	S	B							
partially hydrophobic			B	B	S	S	S	B		T	T	T	T	S	S	S	S	S	B							
fully hydrophobic			&	&	&	&	&	&		T	T	T	T	&	&	&	H	H	H	H	H	H	H			

Designations: H=definite helix, &=probable helix, S=definite strand, B=probable strand, T=possible turn or bend

Table 4. Secondary Structure Prediction for the T4 LYS(11-36) peptide in 0.16 M NaCl, pH 4 at 37°C.

	E	G	L	R	L	K	I	Y	K	D	T	E	G	Y	Y	T	I	G	I	G	H	L	L	T	K	S
aqueous					B	S	S	S	B	B	T	T	T	B	S	S	S	S	B							
partially hydrophobic			B	B	S	S	S	B		T	T	T	T	S	S	S	S	S	B							
fully hydrophobic										T	T	T	T	&	&	&	&	H	H	H	H	H	H			

Designations: H=definite helix, &=probable helix, S=definite strand, B=probable strand, T=possible turn or bend

Table 5. Calculated secondary structure of the T4 LYS(11-36) peptide in 0.16 M NaCl, pH 4 at 25°C (%).

	Fluctuating secondary structure		Fixed secondary structure	
	alpha	beta	alpha	beta
aqueous	6	22	0	46
partially hydrophobic	6	29	0	46
fully hydrophobic	37	7	62	0

Table 6. Calculated secondary structure of the T4 LYS(11-36) peptide in 0.16 M NaCl, pH 4 at 37°C (%).

	Fluctuating secondary structure		Fixed secondary structure	
	alpha	beta	alpha	beta
aqueous	3	20	0	46
partially hydrophobic	4	30	0	46
fully hydrophobic	34	8	38	0

Figure legends

Figure 1. Anisotropy of the T4 LYS(11-36) peptide in pH 4, 25-mM Na-phosphate buffer containing 0.16 M NaCl, as a function of % TFE (v/v); (A) 0% TFE, (B) 10% TFE, (C) 20%TFE, (D) 50% TFE. Symbols represent experimental data at 25°C. Solid lines represent the best-fit curves using Eq. (2).

Figure 2. Anisotropy of the T4 LYS(11-36) peptide in pH 4, 25-mM Na-phosphate buffer containing 0.16 M NaCl, as a function of % TFE (v/v); (A) 0% TFE, (B) 10% TFE, (C) 20%TFE, (D) 50% TFE. Symbols represent experimental data at 37°C. Solid lines represent the best-fit curves using Eq. (2).

Figure 3. Association constant, K_a, for dimerization of the T4 LYS(11-36) peptide at 25°C and 37°C, as a function of % TFE (v/v).

Figure 4. Square-well depth, ε_{spec}, at 25°C and 37°C, as a function of % TFE (v/v).

Figure 5. Far-UV CD spectra of the T4 LYS(11-36) peptide in pH 4, 50-mM Na-phosphate buffer containing 0.16 M NaCl, at 25°C.

Figure 6. Secondary structure from constrained linear regression for the T4 LYS(11-36) peptide in pH 4, 50-mM Na-phosphate buffer containing 0.16 M NaCl, at 25°C.

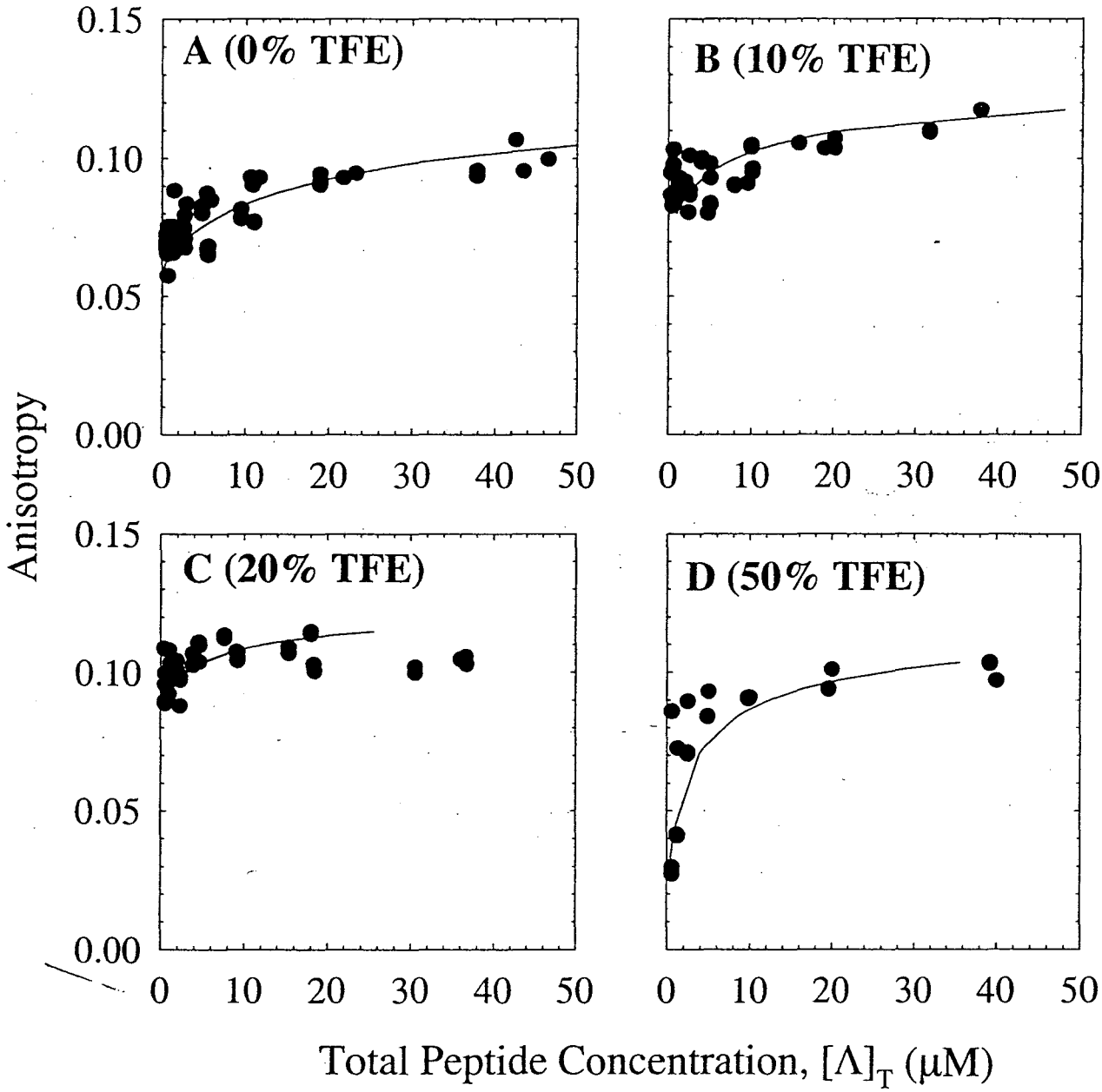

Anderson et al., Figure 1

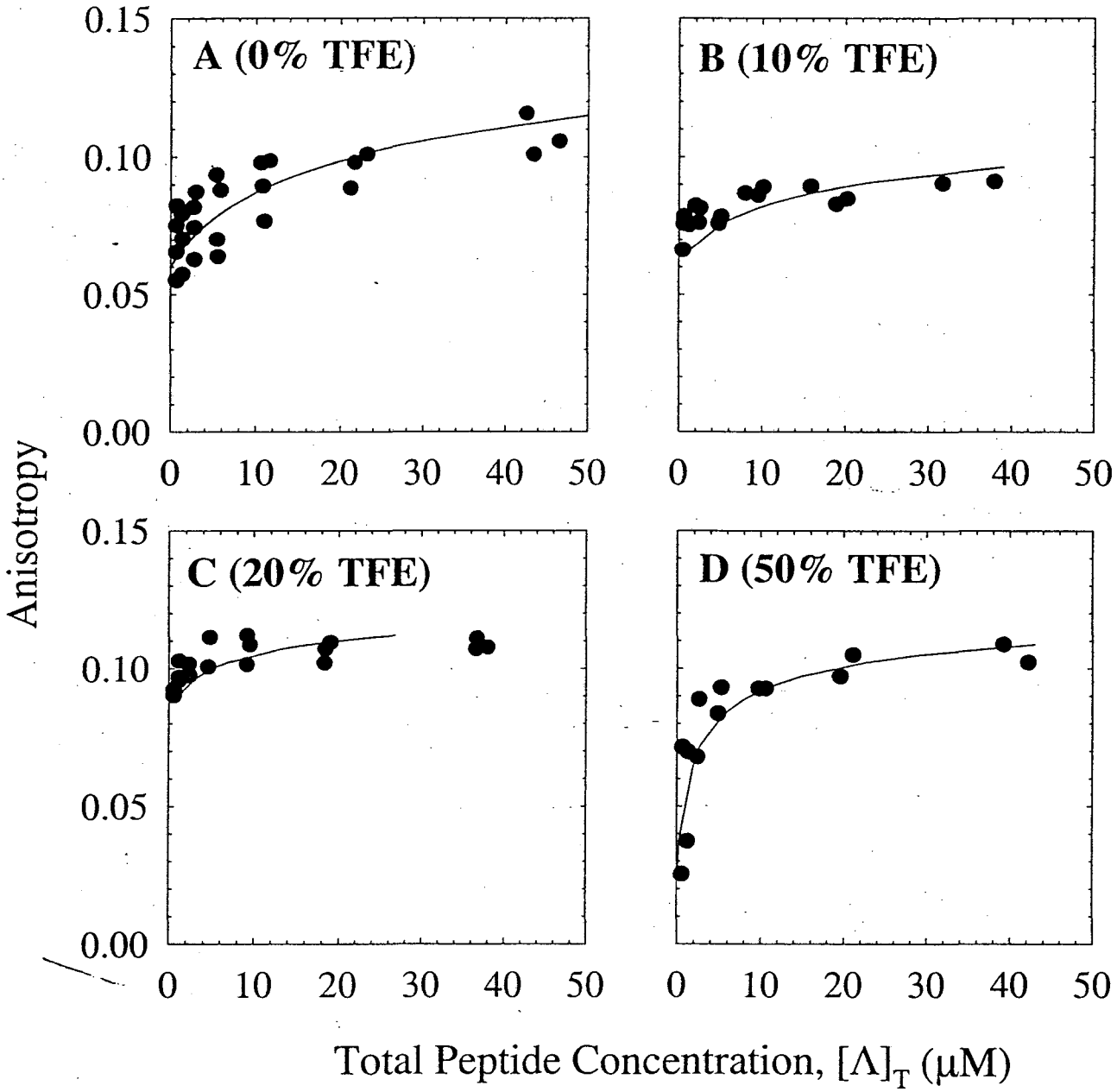

Anderson et al., Figure 2

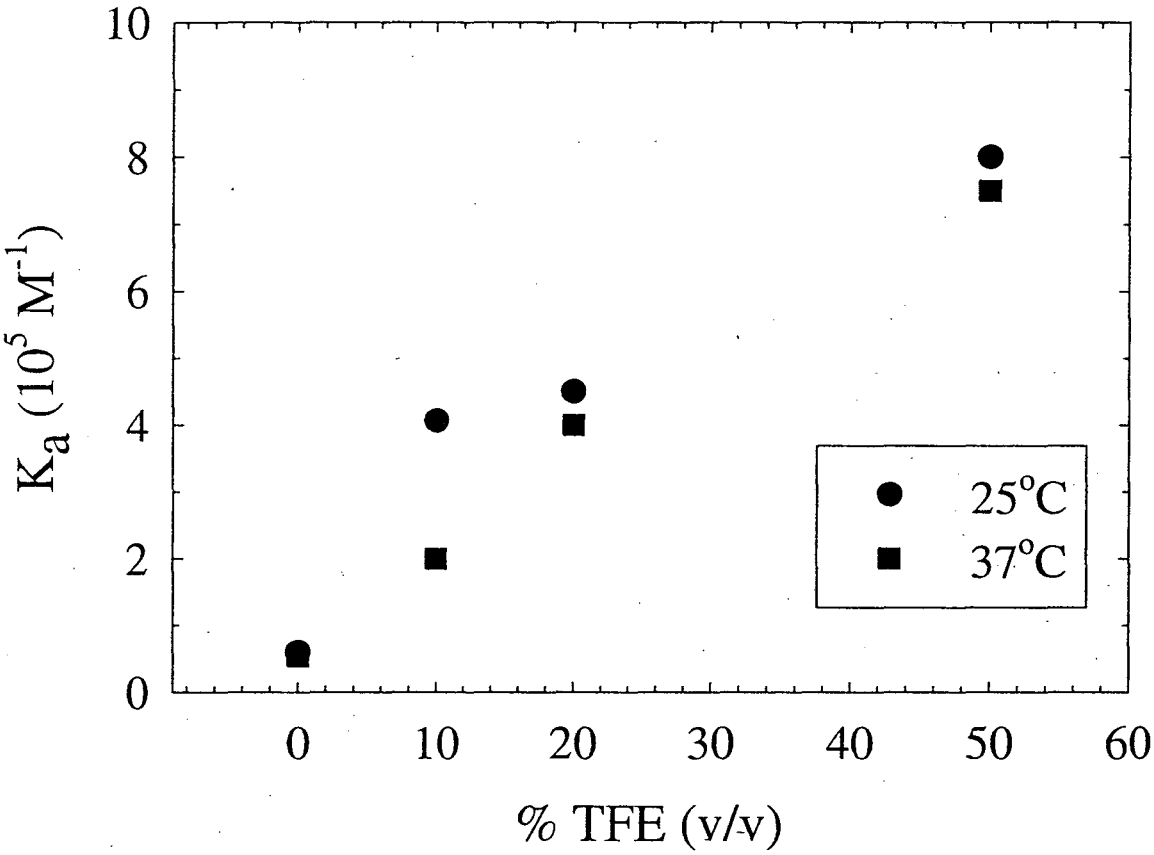

Anderson et al., Figure 3

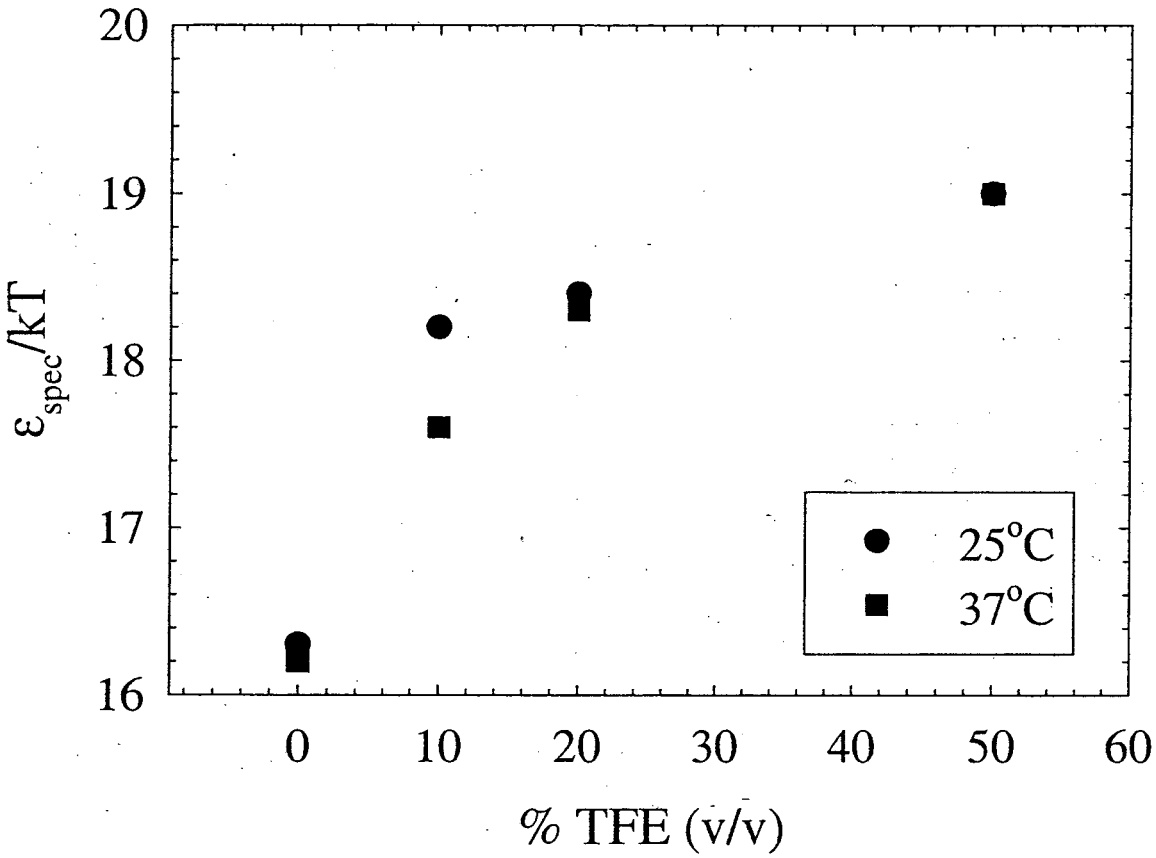

Anderson et al., Figure 4

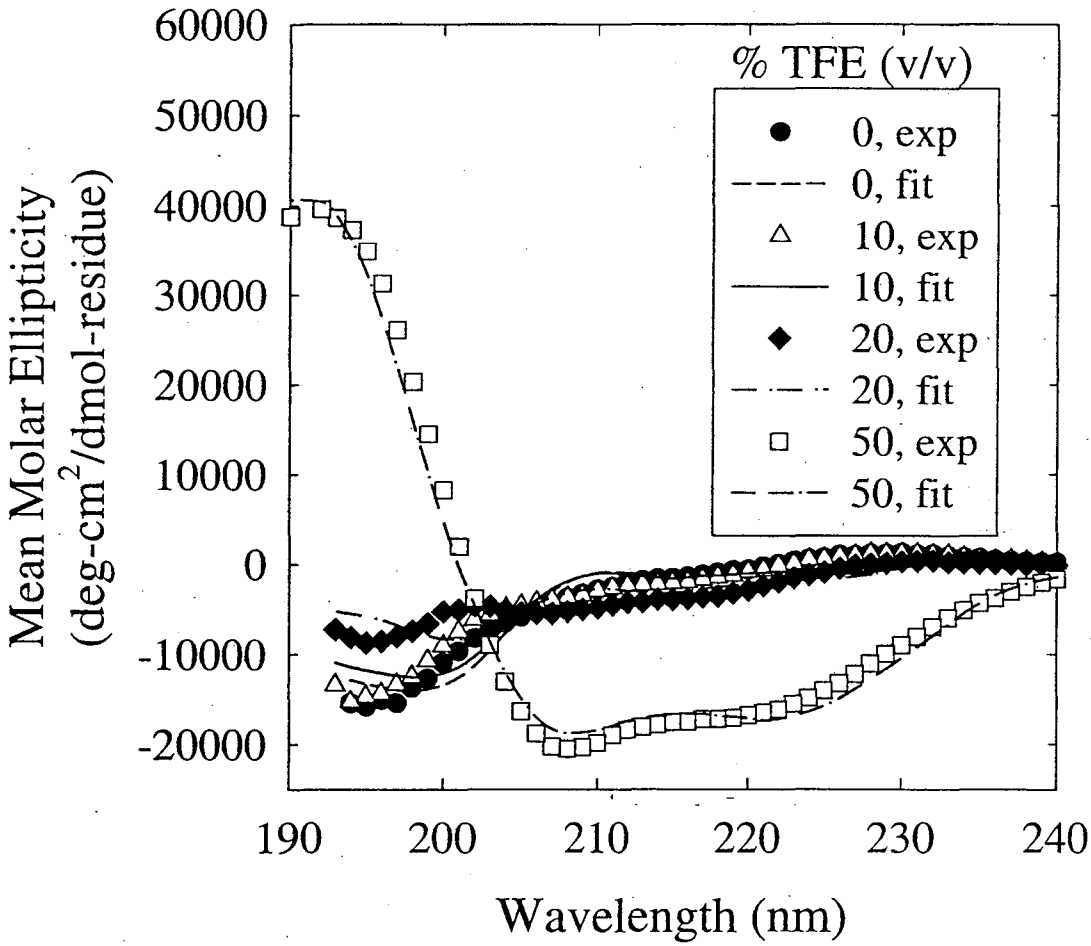

Anderson et al., Figure 5

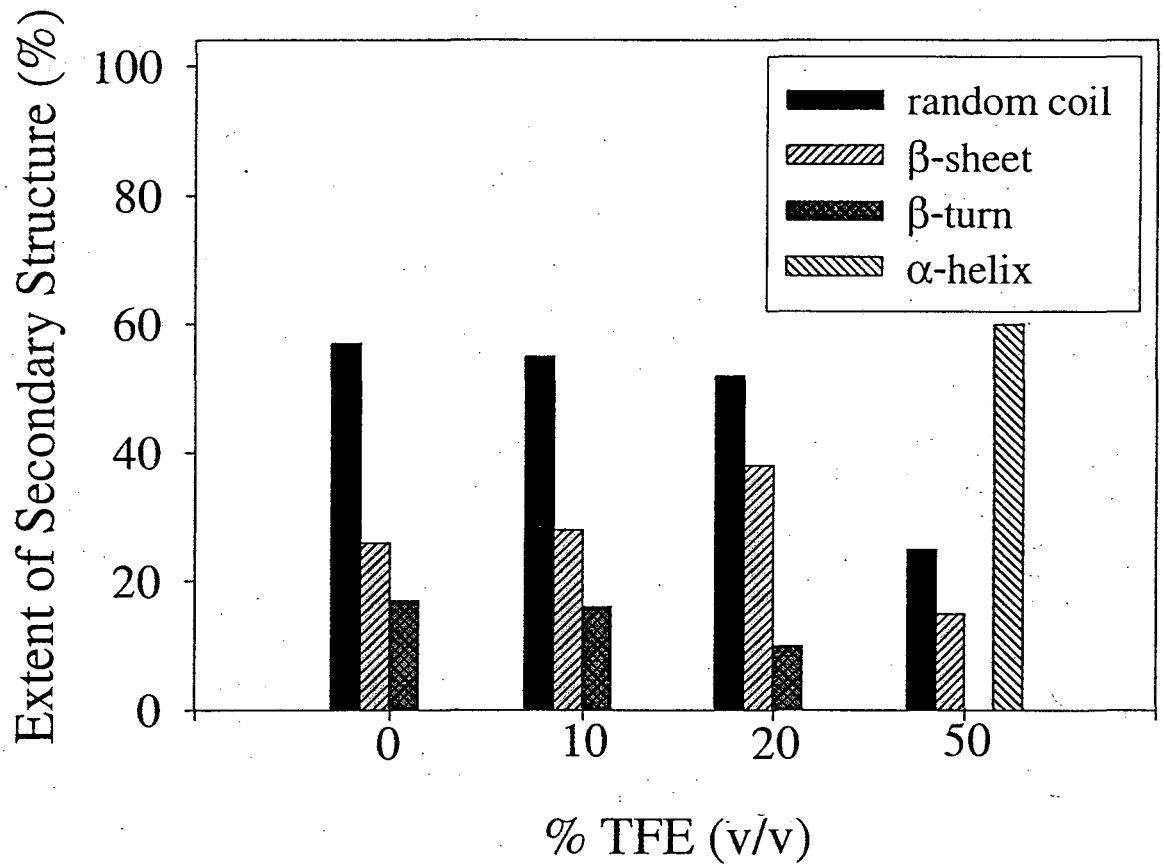

Anderson et al., Figure 6

Ernest Orlando Lawrence Berkeley National Laboratory
One Cyclotron Road | Berkeley, California 94720

Prepared for the U.S. Department of Energy under Contract No. DE-AC03-76SF00098